Biophysical Journal
Article

Biophysical Society

Glycan Determinants of Heparin-Tau Interaction

Jing Zhao,[1,2] Isabelle Huvent,[7] Guy Lippens,[6] David Eliezer,[8] Anqiang Zhang,[2] Quanhong Li,[1] Peter Tessier,[3] Robert J. Linhardt,[2,3,5] Fuming Zhang,[2,*] and Chunyu Wang[2,4,*]

[1]College of Food Science and Nutritional Engineering, China Agricultural University, Beijing, China; [2]Department of Chemistry and Chemical Biology, [3]Department of Chemical and Biological Engineering, [4]Department of Biological Sciences, and [5]Department of Biology and Biomedical Engineering, Center for Biotechnology and Interdisciplinary Studies, Rensselaer Polytechnic Institute, Troy, New York; [6]Laboratoire d'Ingénierie des Systèmes Biologiques et des Procédés, University of Toulouse, CNRS, INRA, INSA, Toulouse, France; [7]Centre National de La Recherche Scientifique-Unité Mixte de Recherche, Université de Lille 1, Villeneuve d'Ascq, France; and [8]Department of Biochemistry, Program in Structural Biology, Weill Cornell Medical College, New York, New York

ABSTRACT Tau aggregates into paired helical filaments within neurons, a pathological hallmark of Alzheimer's disease. Heparin promotes tau aggregation and recently has been shown to be involved in the cellular uptake of tau aggregates. Although the tau-heparin interaction has been extensively studied, little is known about the glycan determinants of this interaction. Here, we used surface plasmon resonance (SPR) and NMR spectroscopy to characterize the interaction between two tau fragments, K18 and K19, and several polysaccharides, including heparin, heparin oligosaccharides, chemically modified heparin, and related glycans. Using a heparin-immobilized chip, SPR revealed that tau K18 and K19 bind heparin with a K_D of 0.2 and 70 μM, respectively. In SPR competition experiments, *N*-desulfation and 2-*O*-desulfation had no effect on heparin binding to K18, whereas 6-*O*-desulfation severely reduced binding, suggesting a critical role for 6-*O*-sulfation in the tau-heparin interaction. The tau-heparin interaction became stronger with longer-chain heparin oligosaccharides. As expected for an electrostatics-driven interaction, a moderate amount of salt (0.3 M NaCl) abolished binding. NMR showed the largest chemical-shift perturbation (CSP) in R2 in tau K18, which was absent in K19, revealing differential binding sites in K18 and K19 to heparin. Dermatan sulfate binding produced minimal CSP, whereas dermatan disulfate, with the additional 6-*O*-sulfo group, induced much larger CSP. 2-*O*-desulfated heparin induced much larger CSP in K18 than 6-*O*-desulfated heparin. Our data demonstrate a crucial role for the 6-*O*-sulfo group in the tau-heparin interaction, which to our knowledge has not been reported before.

INTRODUCTION

The microtubule (MT)-associated protein tau promotes MT assembly and stability in neurons (1,2). It can aggregate into paired helical filaments (PHFs, also called neurofibrillary tangles), a pathological hallmark of Alzheimer's disease (AD) (3,4). The longest mature isoform of tau (Tau 441, 441 residues) consists of several regions: the *N*-terminal projection domain (N1 and N2), the proline-rich region, and the MT binding repeat domain (MTBR) (Fig. 1). MTBR includes four internal sequence repeat motifs (R1–R4) in the C-terminal half of the protein, which is involved in MT binding and tau aggregation (5,6). In fact, MTBR forms PHFs more readily than full-length tau (7). As a consequence, the repeat domain of tau, in the form of tau K18 (with all four repeats) and tau K19 (with three repeats, missing R2 (Fig. 1)) has been used extensively in the study of tau aggregation and interactions.

In vivo, the hyperphosphorylation of tau is thought to induce dissociation of tau from the MT and tau self-aggregation, both of which result in cellular toxicity (8–10). In vitro, the aggregation of tau is triggered by polyanionic agents such as RNA (11), arachidonic acid (12), polyglutamate (13), and heparin (14). Tau is an intracellular protein, whereas glycosaminoglycans (GAGs) such as heparin are on the cell surface or in the extracellular matrix. Under physiological conditions, tau and GAGs would never meet. However, recent work has shown that tau aggregates can spread like prions in the brain. Extracellular tau aggregates can be taken up by neurons and propagated. This uptake is mediated by heparan sulfate and inhibited by heparin (15). Thus, the GAG and tau interaction, besides promoting tau aggregation, figures prominently in the tau pathology of AD.

Heparin is a linear, polydisperse, and highly sulfated GAG that exhibits numerous biological activities (16–18).

Submitted October 25, 2016, and accepted for publication January 26, 2017.

*Correspondence: zhangf2@rpi.edu or wangc5@rpi.edu

Editor: Daniel Raleigh.

http://dx.doi.org/10.1016/j.bpj.2017.01.024

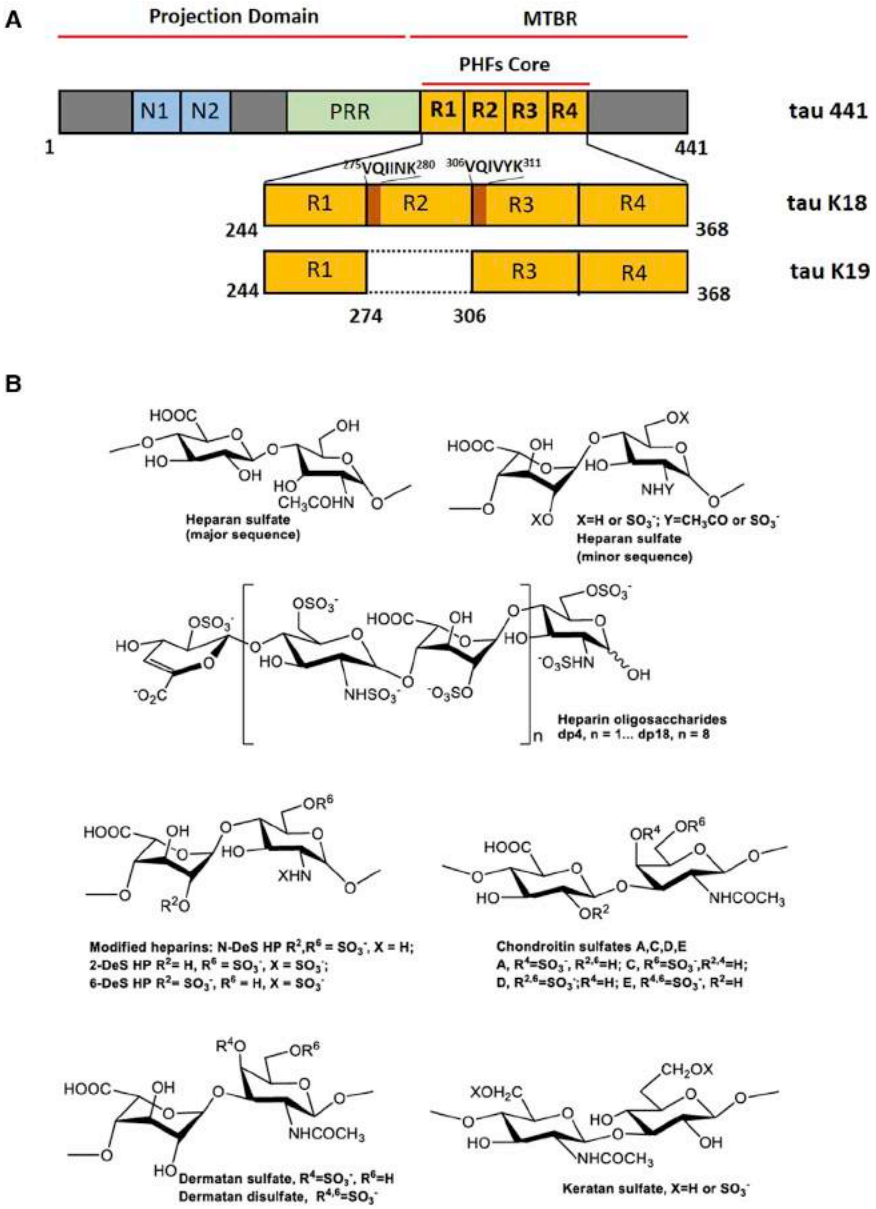

FIGURE 1 Tau constructs and GAGs used in this study. (*A*) Tau K18 and K19. The C-terminal half of tau 441, which is the longest tau isoform in the human central nervous system, contains four repeats (R1–R4, *orange shade*). The constructs K18 and K19 comprise four repeats and three repeats, respectively. The residue numbering is based on the numbering of tau 441. (*B*) Chemical structures of heparin, heparin-derived oligosaccharides, chemically modified heparin, and other GAGs. To see this figure in color, go online.

It has complex microheterogeneity due to the numerous structural variations in its disaccharide units. The 2-amino group of the glucosamine residue, the 3- and 6-hydroxyl groups of the glucosamine residues, and the 2-hydroxyl group of the iduronic or glucuronic acid residues can all be substituted with sulfo groups (Fig. 1) (19).

The interaction between tau and heparin has been well studied and seems to be driven by electrostatic interactions. Chemical-shift perturbations (CSPs) in the NMR spectrum of tau upon addition of heparin identified positively charged lysine and histidine as the hot spots of binding (20,21). The hexapeptide ^{275}VQIINK^{280} in the beginning of the second repeat domain (R2) was found to bind heparin and plays a crucial role in tau aggregation (22). Mature tau has 44 lysine residues out of 441 residues with a theoretical pI of 8.24, and heparin likely enhances aggregation of tau by reducing the electrostatic repulsion between tau monomers.

Only a few studies have addressed the glycan determinants of the heparin-tau interaction, such as the effects of specific sulfation patterns and oligosaccharide chain lengths (23,24). In this study, surface plasmon resonance (SPR) and NMR spectroscopy were utilized to characterize the interaction between two tau constructs, tau K18 and tau K19, and heparin and related GAGs. A heparin-immobilized streptavidin (SA) chip was used to directly analyze the kinetics of binding using SPR. SPR competition between the heparin on the chip and GAGs in the solution phase was conducted to indirectly characterize the glycan determinants involved in this interaction. In addition, NMR titration was applied to directly identify binding sites on tau and to confirm the SPR findings. Intriguingly, our data demonstrate that the

6-*O*-sulfo group in heparin plays a crucial role in the tau-heparin interaction.

MATERIALS AND METHODS

Materials

Tau K18 (25) and tau K19 (26) were prepared as previously described. Heparin with an average molecular mass of 15 kDa and polydispersity of 1.4 was purchased from Celsus Laboratories (Cincinnati, OH), where it was extracted and purified from porcine intestine. *N*-desulfated heparin (14 kDa) and 2-*O*-desulfated IdoA heparin (13 kDa) were prepared according to Yates et al. (27). A 6-*O*-desulfated heparin (13 kDa) was provided by Dr. Liangchun Wang from the University of Georgia. The GAGs used were porcine intestinal heparan sulfate (12 kDa, Celsus Laboratories), chondroitin sulfate A (20 kDa) from porcine rib cartilage (Sigma, St. Louis, MO), dermatan sulfate (DS; also known as chondroitin sulfate B, 30 kDa, from porcine intestine; Sigma), chondroitin sulfate C (20 kDa, from shark cartilage; Sigma), chondroitin sulfate D (20 kDa, from shark cartilage; Seikagaku, Tokyo, Japan), chondroitin sulfate E (20 kDa, from squid cartilage; Seikagaku), and keratan sulfate (14.3 kDa) that was isolated from bovine cornea (28). The heparin oligosaccharides included tetrasaccharide (dp4), hexasaccharide (dp6), octasaccharide (dp8), decasaccharide (dp10), dodecasaccharide (dp12), tetradecasaccharide (dp14), hexadecasaccharide (dp16), and octadecasaccharide (dp18), and were prepared by controlled partial heparin lyase 1 treatment of bovine lung heparin (Sigma) followed by size fractionation (29). The chemical structures of these GAGs are shown in Fig. 1. Sensor SA chips were obtained from GE Healthcare Bio-Sciences AB (Uppsala, Sweden). SPR measurements were performed on a BIAcore 3000 operated using BIAcore 3000 control and BIAevaluation software (version 4.0.1).

Preparation of the heparin biochip

Biotinylated heparin was prepared by reacting sulfo-*N*-hydroxysuccinimide long-chain biotin (Thermo Scientific, Waltham, MA) with free amino groups of unsubstituted glucosamine residues in the polysaccharide chain according to a published procedure (30). The biotinylated heparin was immobilized to an SA chip based on the manufacturer's protocol. In brief, a 20 mL solution of the heparin-biotin conjugate (0.1 mg/mL) in HBS-EP running buffer (0.01 M HEPES, 0.15 M NaCl, 3 mM EDTA, and 0.005% surfactant P20 (pH 7.4)) was injected over flow cell 2 (FC2) of the SA chip at a flow rate of 10 μm/min. Successful immobilization of heparin was confirmed by the observation of an ~250 resonance unit increase in the sensor chip. The control flow cell (FC1) was prepared by a 1 min injection with saturated biotin.

SPR of the binding between heparin and tau

The lyophilized tau K18/K19 protein samples were resuspended in HBS-EP buffer. Different dilutions of the protein samples were injected at a flow rate of 30 μL/min. At the end of the sample injection, the same buffer was flowed over the sensor surface to facilitate dissociation. After a 3 min dissociation time, the sensor surface was regenerated by injection with 30 μL of 2 M NaCl. The response was monitored as a function of time (sensorgram) at 25°C.

Solution competition study between heparin on the chip surface and chemically modified heparin/DS in solution

Competition SPR experiments using chemically modified heparin and DS were performed to study the tau-heparin interaction and test how the degree of sulfation and the position of sulfo groups in GAGs impact tau binding. Tau K18 was separately premixed with 1 μM of chemically modified heparin or DS and injected over the heparin chip at a flow rate of 30 μL/min. After each injection and association, dissociation and regeneration were performed as described above. For each set of competition experiments on SPR, a control experiment (with only protein and no GAG or oligosaccharide in solution) was performed to confirm that the surface was completely regenerated and that the results obtained between runs were comparable. All data are based on triplicate experiments and double reference subtracted. The standard deviation was calculated from three replicates.

Solution competition study between heparin on the chip surface and GAGs in solution

Tau K18 and Tau K19 were premixed with 1 μM of GAG separately and injected over the heparin chip at a flow rate of 30 μL/min to evaluate the competition of another GAG with the tau-heparin interaction. After each injection and association, dissociation and regeneration were performed as described above. For each set of competition experiments on SPR, a control experiment (with only protein without any GAG or oligosaccharide) was performed to confirm that the surface was completely regenerated and that the results obtained between runs were comparable. All data are based on triplicate experiments and double reference subtracted. The standard deviation was calculated from three replicates.

Solution competition study between heparin on the chip surface and heparin-derived oligosaccharides in solution

Tau K18 and tau K19 were mixed with 1 μM of heparin oligosaccharides (including dp4, dp6, dp8, dp10, dp12, dp14, dp16, and dp18 in HBS-EP buffer) and injected over the heparin chip at a flow rate of 30 μL/min. After each run, dissociation and regeneration steps were performed as described above. For each set of competition experiments on SPR, a control experiment (with only protein and no GAG or oligosaccharide in solution) was performed to confirm that the surface was completely regenerated and that the results obtained between runs were comparable. All data are based on triplicate experiments and double reference subtracted. The standard deviation was calculated from three replicates.

Effect of salt concentration on the interaction between heparin and tau

Tau K18 and tau K19 were diluted in HBS-P buffer (0.01 M HEPES, 0.15 M NaCl, and 0.005% surfactant P20 (pH 7.4)) with different NaCl concentrations and injected at a flow rate of 30 μL/min. At the end of the sample injection, the same buffer was flowed over the sensor surface to facilitate dissociation. After a 3 min dissociation time, the sensor surface was regenerated by injecting 30 μL of 2 M NaCl. The response was monitored as a function of time (sensorgram) at 25°C. All data are based on triplicate experiments and double reference subtracted. The standard deviation was calculated from three replicates.

NMR titration of tau K18/K19 with full-length heparin

NMR spectra of tau K18 and K19 were acquired at 10°C on an 800 MHz NMR spectrometer (Bruker, Billerica, MA) equipped with a cryogenic probe. Aggregation did not occur at this low temperature. The NMR data were processed and analyzed using Topspin 2.1.6 and Sparky. Tau K18 was prepared based on the method described by Barré and Eliezer (25).

^{15}N-labeled tau K18 was dissolved in 100 mM NaCl, 10 mM Na_2HPO_4, and 4 mM dithiothreitol at pH 7.4 in 90/10% H_2O/D_2O, and the tau K19 sample was dissolved in the same buffer but without dithiothreitol (26). A series of ^{1}H-^{15}N heteronuclear single quantum coherence (HSQC) experiments were performed on a 0.1 mM tau sample by adding increasing amounts of heparin lyophilized aliquots. Normalized, weighted average CSPs for amide ^{1}H and ^{15}N chemical shifts upon heparin addition were calculated using the equation $\Delta\,\delta = \sqrt{100\Delta H^2 + \Delta N^2}$, where ΔH and ΔN are the differences between the ^{15}N and ^{1}H chemical shifts of the free and bound forms of tau protein, respectively.

NMR titration of tau K18 with 6-Des HEP and 2-Des HEP

Titration experiments with 6-*O*-desulfated heparin (6-Des HEP) and 2-*O*-desulfated heparin (2-Des HEP) were performed on tau K18 to further understand the specific effect of the 6-*O*-sulfo group on tau binding using two chemically modified heparin samples with similar charge densities. A series of separate ^{1}H-^{15}N HSQC spectroscopy experiments were performed on a 0.1 mM tau sample by adding increasing amounts of 6-Des HEP and 2-Des HEP lyophilized aliquots. Normalized, weighted average chemical-shift differences for amide ^{1}H and ^{15}N chemical shifts upon heparin addition were calculated using the equation $\Delta\,\delta = \sqrt{100\Delta H^2 + \Delta N^2}$, where ΔH and ΔN are the differences between the chemical shifts of the free and bound forms of tau protein, respectively.

NMR titration of tau K18 with DS and Dermatan Disulfate

Titration experiments with DS and dermatan disulfate (Dis-DS), which differ only at their C6 position of GalNac residue substitution (Fig. 1), were performed on tau K18 to examine the effect of the 6-*O*-sulfo group in other GAGs on tau binding. A series of separate ^{1}H-^{15}N HSQC spectroscopy experiments were performed on a 0.1 mM tau sample by adding increasing amounts of DS and Dis-DS lyophilized aliquots. Normalized, weighted average chemical-shift differences for amide ^{1}H and ^{15}N chemical shifts upon heparin addition were calculated using the equation $\Delta\,\delta = \sqrt{100\Delta H^2 + \Delta N^2}$, where ΔH and ΔN are the differences between the chemical shifts of the free and bound forms of tau protein, respectively. In an NMR competition experiment, 0.1 mM tau K18 was titrated with DS and then Dis-DS was added. Finally, 0.1 mM heparin was added to the same sample after the DS-tau sample was titrated by Dis-DS. The chemical-shift changes of the residues were observed along with the competitive titration.

RESULTS AND DISCUSSION

The heparin chip shows a higher binding affinity for K18 than for K19

Heparin has been reported to accelerate the in vitro aggregation of tau (13,14). Kinetic measurements of the heparin-tau interaction were carried out using a sensor chip immobilized with heparin (Fig. 2). The sensorgrams of tau K18 and tau K19 displayed different shapes, indicating their different binding affinities to heparin. Both sets of binding curves fit well with the 1:1 Langmuir binding model, consistent with a monophasic-binding process. The apparent on-rate (k_{on}) of tau K18-heparin binding is significantly greater than that of tau K19, whereas the apparent off-rate (k_{off}) is smaller (Fig. 2). The K_D was calculated to be 2.0×10^{-7} M for the tau K18-heparin interaction, which is stronger than the K_D calculated for the tau K19-heparin interaction (7.1×10^{-5} M), indicating a crucial role for R2, which is absent in K19. This is consistent with the report of Mukrasch et al. (22), who identified a region at the beginning of the R2 domain as the key heparin-binding site.

Competition SPR revealed the crucial role of the 6-*O*-sulfo group

Although the binding between tau and heparin has been extensively studied from the protein side, little is known

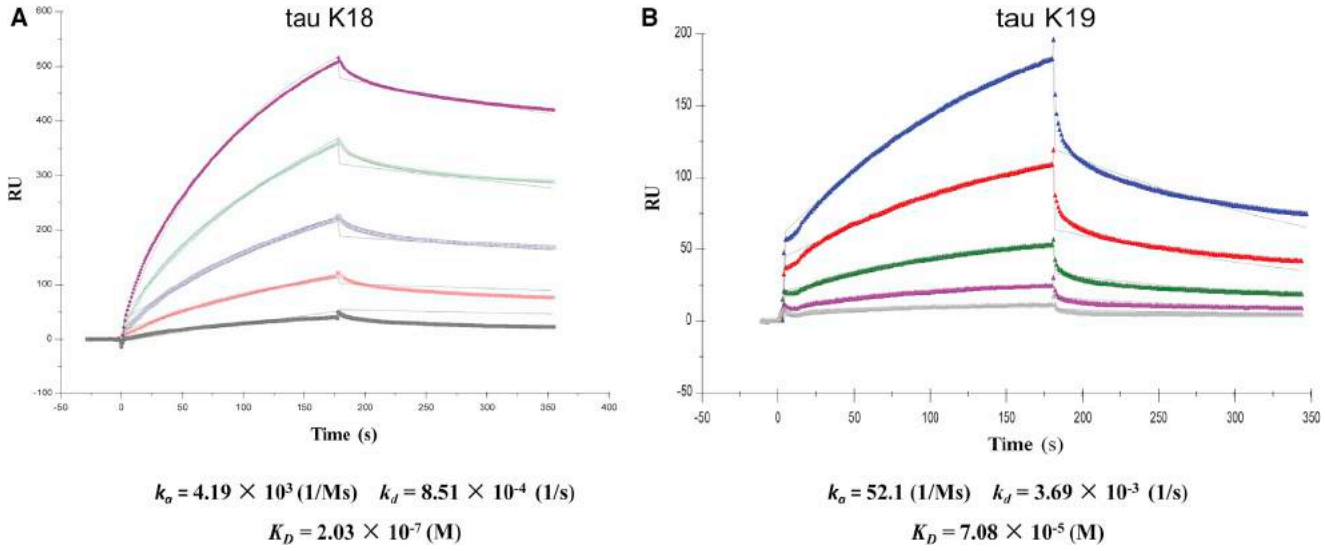

FIGURE 2 SPR shows that tau K18 binds heparin with higher affinity than K19. (*A*) SPR sensorgrams and binding affinity of the tau K18-heparin interaction. The concentrations of the protein (from *top* to *bottom*) were 2.0, 1.0, 0.5, 0.25, and 0.125 μM, respectively. (*B*) SPR sensorgrams and binding affinity of the tau K19-heparin interaction. The concentrations of the protein (from *top* to *bottom*) were 32, 16, 8, 4, and 2 μM, respectively. The black curves are the fit curves using models from BIAevaluation 4.0.1. To see this figure in color, go online.

about the structural requirements on the heparin side for binding to tau. We performed solution/surface competition experiments using SPR to examine the effects of the sulfation pattern and the chain size of heparin and other GAGs on the heparin-tau interaction. Briefly, in this approach, SPR is performed using the heparin chip with tau preincubated with various GAGs in solution. Once the heparin-binding sites in tau are occupied by GAG in the solution, tau binding to the surface-immobilized heparin should decrease, resulting in a reduction in the magnitude of the SPR signal. This well-established method has been used in many previous studies to characterize the heparin-protein interaction (31–33).

Sulfation pattern

Competition SPR experiments using chemically modified heparin and DS were performed to investigate the effect of the GAG sulfation pattern on binding to tau K18 (Fig. 3). *N*-Des HEP, 6-Des HEP, and 2-Des HEP are abbreviations for *N*-desulfated heparin, 6-*O*-desulfated heparin, and 2-*O*-desulfated heparin, respectively. DS is sulfated only at the C4 position of GalNAc residues, whereas Dis-DS is sulfated at both the C4 and C6 positions, as shown in Fig. 1. As expected, heparin in solution suppressed SPR binding to ~25% of that observed with the control (Fig. 3). The removal of 6-*O*-sulfo groups from heparin (6-Des HEP) markedly weakened the ability of this modified heparin to compete with surface-immobilized heparin for tau K18 binding. In contrast, the removal of 2-*O*-sulfo and *N*-sulfo groups did not affect the competition, indicating that the 6-*O*-sulfo group is much more important for the tau-heparin interaction than 2-*O*- and *N*-sulfation. DS, with only a 4-*O*-sulfo group, can prevent 50% of the K18 binding to the chip. Dis-DS, with the addition of a 6-*O*-sulfo group, competes better than DS, but the increased competition is less than that observed with heparin. Thus, the 6-*O*-sulfo group may not be as important for other GAGs in the tau interaction.

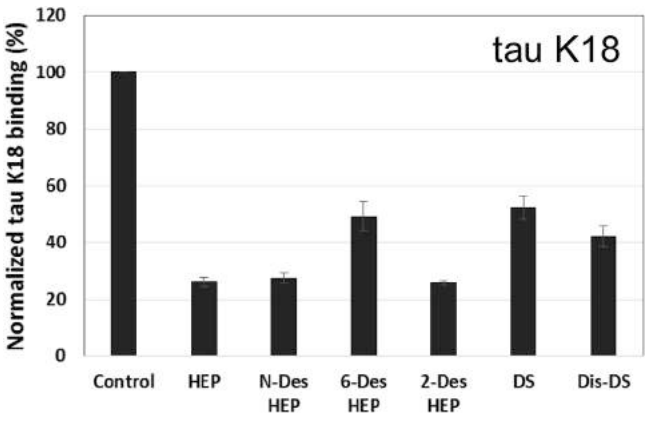

FIGURE 3 SPR competition indicates the importance of 6-*O*-sulfation. The normalized SPR signal of tau K18-heparin binding is shown in the presence of different chemically modified samples of heparin and DS in solution. The tau K18 concentration was 0.5 μM and the concentration of the modified heparin/DS in solution was 1 μM. All bar graphs are based on triplicate experiments.

Other GAGs

The SPR competition assay was also utilized to determine the binding preference of tau K18/K19 to naturally occurring GAGs other than heparin (Fig. 4). These GAGs have different chain lengths, which makes it hard to compare their affinities. For both tau K18 and tau K19, heparin produced the strongest inhibition by competing for 74% and 60% of the binding signal, respectively. Apart from heparin, chondroitin sulfate E (CSE) showed the highest inhibitory activity (57% for K18 and 33% for K19), followed by DS (48% for K18 and 28% for K19). For tau K18, modest inhibitory activities (>20%) were observed for CSC. Weak inhibitory activity was observed for chondroitin sulfate A (CSA), chondroitin sulfate D (CSD), and keratin

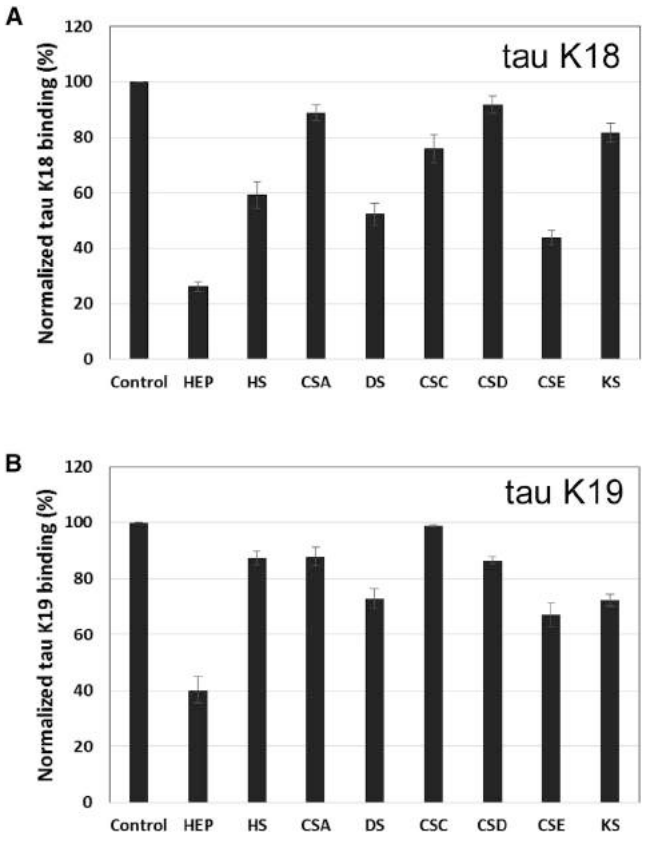

FIGURE 4 Tau K18/K19 binding to various GAGs characterized by SPR competition. The best competitor in the SPR competition assay, CSE, also contains 6-*O*-sulfate. (*A*) Bar graphs of the normalized SPR signal of tau K18 binding to surface heparin in the presence of different GAGs in solution. The tau K18 concentration was 0.5 μM and the concentration of the GAGs in solution was 1 μM. (*B*) Bar graphs of the normalized SPR signal of tau K19 binding to surface heparin in the presence of different GAGs in solution. The tau K19 concentration was 16 μM and the concentration of the GAGs in solution was 1 μM. All bar graphs are based on triplicate experiments.

sulfate (KS). For tau K19, KS also showed modest inhibitory activities (>20%) and CSA, CSD, and heparin sulfate (HS) showed very weak inhibitory activity.

The data show that the inhibitory effects of GAGs on the tau−immobilized heparin interaction were greatest for heparin with 2.8 mol of sulfate per disaccharide repeating unit, followed by CSE with 1.5−2 mol of sulfate per disaccharide, then HS with 1.2 mol of sulfate per disaccharide, and finally DS, CSA, and CSC with <1 mol of sulfate per disaccharide. Surprisingly, CSD with 1.5−2 mol of sulfate per disaccharide showed a comparable level of competition with GAGs having <1 mol of sulfate per disaccharide, likely due to distribution of the two sulfo groups to two separate monosaccharides. These results indicate that tau K18 and K19 prefer more highly sulfated GAGs, further demonstrating that an electrostatic interaction is the driving force for this interaction. In addition, the geometry of the sulfate distribution is also found to be important for the GAG-tau interaction. This behavior of tau protein is similar to the GAG preference for other proteins, such as langerin (31), adeno-associated virus (32), and fibroblast growth factor (33).

Chain size

Heparin-derived oligosaccharides of different sizes (dp4–dp18; Fig. 1) were used for the SPR competition assay. For tau K18, the binding signal of tau to the surface heparin decreased gradually as the chain length of the competing oligosaccharide increased, indicating that longer oligosaccharides compete better with the heparin chip for tau binding. When the size of the oligosaccharide increased to dp18, the binding of tau K18 to the surface heparin decreased by 49% (Fig. 5 *A*). Similar results were observed for tau K19 (Fig. 5 *B*), although the effect of chain size was not as evident as that seen for K18. No inhibitory effect was found from dp4 to dp8. As the chain length increased further beyond dp8, the tau-heparin (surface) binding began to be inhibited. The highest competition level of 20% was observed when the size of the oligosaccharide was dp18. The minimal heparin chain-length requirements for tau K18 and tau K19 are dp6 and dp10, respectively. These results confirm that the interaction between tau K18/K19 and heparin is chain-length dependent and that tau K18/K19 prefers to bind longer-chain heparin oligosaccharides (24). The underlying mechanism of the observed chain-length dependence is likely due to the increased number of sulfate and negative charges in the longer GAG molecules, consistent with the idea that an electrostatic interaction is the driving force of the tau-GAG interaction.

Dependence of the interaction between heparin and tau on salt concentration

Binding buffers with different salt (NaCl) concentrations (0.15 M as control, and 0.3, 0.5, and 1 M) were used in SPR experiments (Fig. 6). Moderate salt concentrations

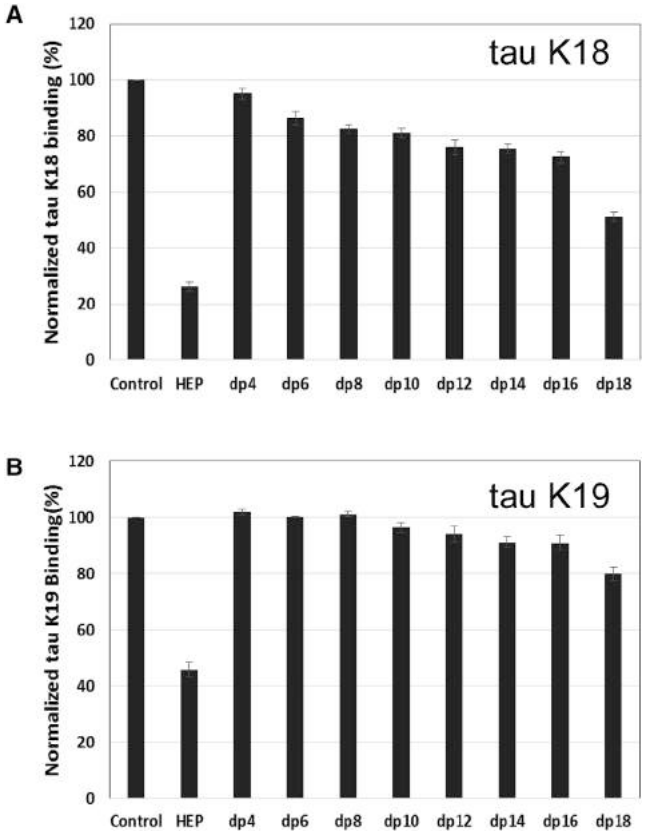

FIGURE 5 Glycan chain-length dependence of the tau-heparin interaction. (*A*) Bar graphs of the normalized signal of tau K18 binding to immobilized heparin in the presence of different chain lengths of heparin-oligosaccharides in solution. The tau K18 concentration was 0.5 μM and the concentration of the heparin oligosaccharides in solution was 1 μM. (*B*) Bar graphs of the normalized SPR signal of tau K19 binding to immobilized heparin in the presence of different chain lengths of heparin-oligosaccharides in solution. The tau K19 concentration was 16 μM and the concentration of the heparin oligosaccharides in solution was 1 μM. All bar graphs are based on triplicate experiments.

(0.3 M) almost completely suppressed tau binding to heparin for both K18 and K19, confirming that the tau-heparin interaction is primarily an electrostatically driven process (20,34).

NMR showed different tau-binding sites for K18 and K19

Numerous NMR studies have characterized the tau-ligand interaction and tau itself, an intrinsically disordered protein (25,26,35–39). In this study, GAG titrations were performed on ^{15}N-labeled tau K18 and tau K19 monomers at 10°C.

Significant CSPs were observed for both tau K18 and tau K19 with the addition of heparin (Fig. 7, *A* and *B*). For tau K18, little additional CSP was observed above the molar ratio of 1:1 (heparin/tau K18). The largest CSPs were found in the R2 domain, especially for I277-D283 at the beginning of R2. The hexapeptide ^{275}VQIINK^{280} in R2, which governs tau aggregation and binds MT, has been identified as the main site of contact with heparin (37). In our hands, the downstream residues (K281, L282, and D283) showed more pronounced CSPs than the hexapeptide ^{275}VQIINK^{280} (Fig. 7 *E*). Two

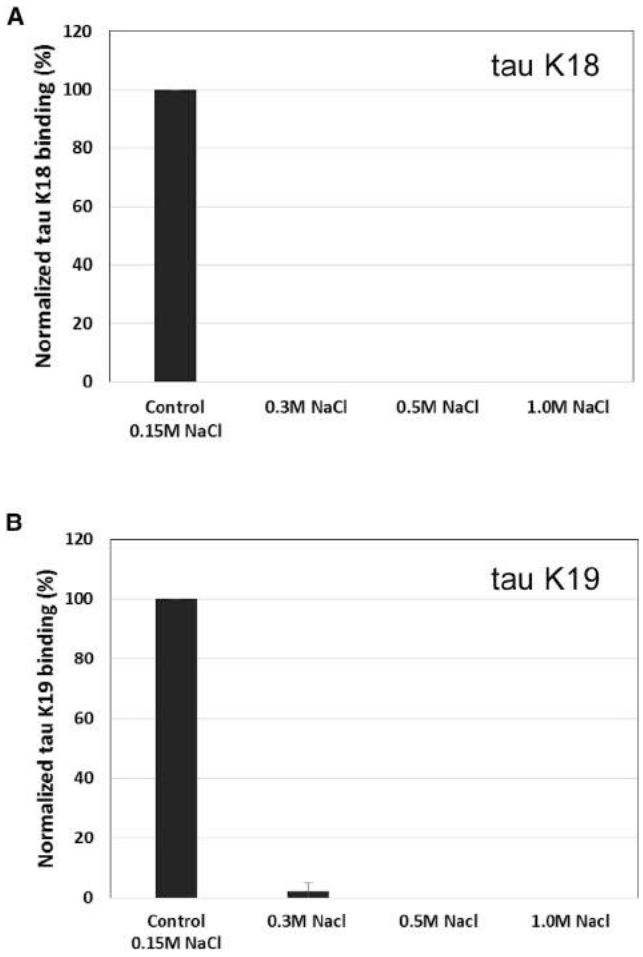

FIGURE 6 Salt dependence of the tau-heparin interaction. (*A*) Binding of tau K18 to heparin at various NaCl concentrations. (*B*) Binding of tau K19 to heparin at various NaCl concentrations. The tau K18 concentration was 0.5 μM and the tau K19 concentration was 16 μM. All bar graphs are based on triplicate experiments. To see this figure in color, go online.

hydrophobic amino acids, I278 and L282, displayed the largest shift, which could be due to a conformational rearrangement that exposes the side chain of these two hydrophobic residues to seed aggregation and promote intermolecular interactions. In addition, strong CSPs were observed for many lysine residues, including K254, K290, K294, and K298, again confirming the electrostatic nature of tau-heparin binding. A similar CSP pattern was observed on tau K18 with a low-molecular-mass heparin (3000 kDa) (20). Significant CSPs were also observed for E264-N265, N286, H268-Q269, Q351, T319, T361, V339, V337, and L253.

For tau K19, near saturation in CSP was not reached until a 1:3 (tau K19/heparin) molar ratio, reflecting the lower binding affinity of tau K19 to heparin (Fig. 7, *C* and *D*) as measured by SPR. The CSP magnitude was smaller for K19 at the same tau/heparin ratio and the overall CSP pattern was significantly different. In the absence of R2, V306-K311 in R3 showed large CSPs, and the Y310 residue was shown to be important for maintaining the rigid extended structure of ^{306}VQIVYK^{311}, which is essential for tau aggregation (40). In addition, the clusters of positively charged residues upstream of the PGGG motif (K267-Q269 in R1, H329-K331 in R3, and H362-V363 in R4) showed large CSPs. These regions were also the major MT binding sites of tau (19). Other positively charged areas, such as K254-K257, K317-V318, and Q351-K353 in the middle of R1, R3, and R4, respectively, experienced significant CSPs as well. In addition, V339, E342, and L344 flanking the Lys residues at the beginning of R4 showed CSPs.

NMR titration confirms the role of 6-*O*-sulfation in tau binding

To further demonstrate the importance of 6-*O*-sulfation as revealed by SPR, an NMR titration experiment was performed on ^{15}N-labeled tau K18 with 6-Des HEP and 2-Des HEP, whose charge densities are identical. This allowed us to directly compare the roles of 2-*O*-sulfo and the 6-*O*-sulfo group in tau binding. Very small CSPs were observed after 0.2 mM 6-Des HEP was added to the 0.1 mM tau K18 solution, although the CSPs of I277-L282 and K290 in R2 could still be detected (Fig. 8, *A* and *B*). In contrast, titration of 0.2 mM 2-Des HEP to 0.1 mM tau K18 generated much larger CSPs over more residues (Fig. 8, *C* and *D*). The large CSP difference between 6-Des HEP and 2-Des HEP corroborate the SPR competition data in Fig. 3 and confirm the crucial role of 6-*O*-sulfation in the tau-heparin interaction, which to our knowledge has never been identified before. The CSP pattern induced by 2-Des HEP is close to that induced by heparin (Fig. 8 *E*), suggesting that 2-*O*-sulfation is not as important as 6-*O*-sulfation in the tau-heparin interaction.

NMR titration performed on ^{15}N-labeled tau K18 with DS (with only 4-*O*-sulfation of GalNAc) and Dis-DS (with both 4-*O*-sulfation and 6-*O*-sulfation of GalNAc, which is structurally similar to CSE) further confirmed the influence of the 6-*O*-sulfation pattern on binding. Similar to the case with 6-Des HEP, small CSPs were observed after 0.1 mM DS was added to the 0.1 mM tau K18 solution (Fig. 9, *A* and *B*). Addition of Dis-DS to the same sample generated much larger CSPs over more residues (Fig. 9, *C* and *D*), confirming that Dis-DS showed better SPR competition than DS (Fig. 3). The CSP pattern of Dis-DS is similar to that of heparin, suggesting that heparin and Dis-DS share similar tau-binding sites.

Finally, as shown in Fig. 9 *E*, we carried out NMR competition experiments with DS, Dis-DS, and heparin. First, DS was titrated into a tau NMR sample (0.1 mM) to near saturation at a molar ratio of 1:1. Further significant CSPs were observed upon addition of Dis-DS (to 0.1 mM) to the tau sample that was already titrated with DS, and adding heparin to 0.1 mM induced further CSPs in the DS and Dis-DS titrated tau samples. These NMR data confirm the order of tau binding affinity observed in SPR, that is, heparin $>$ Dis-DS $>$ DS.

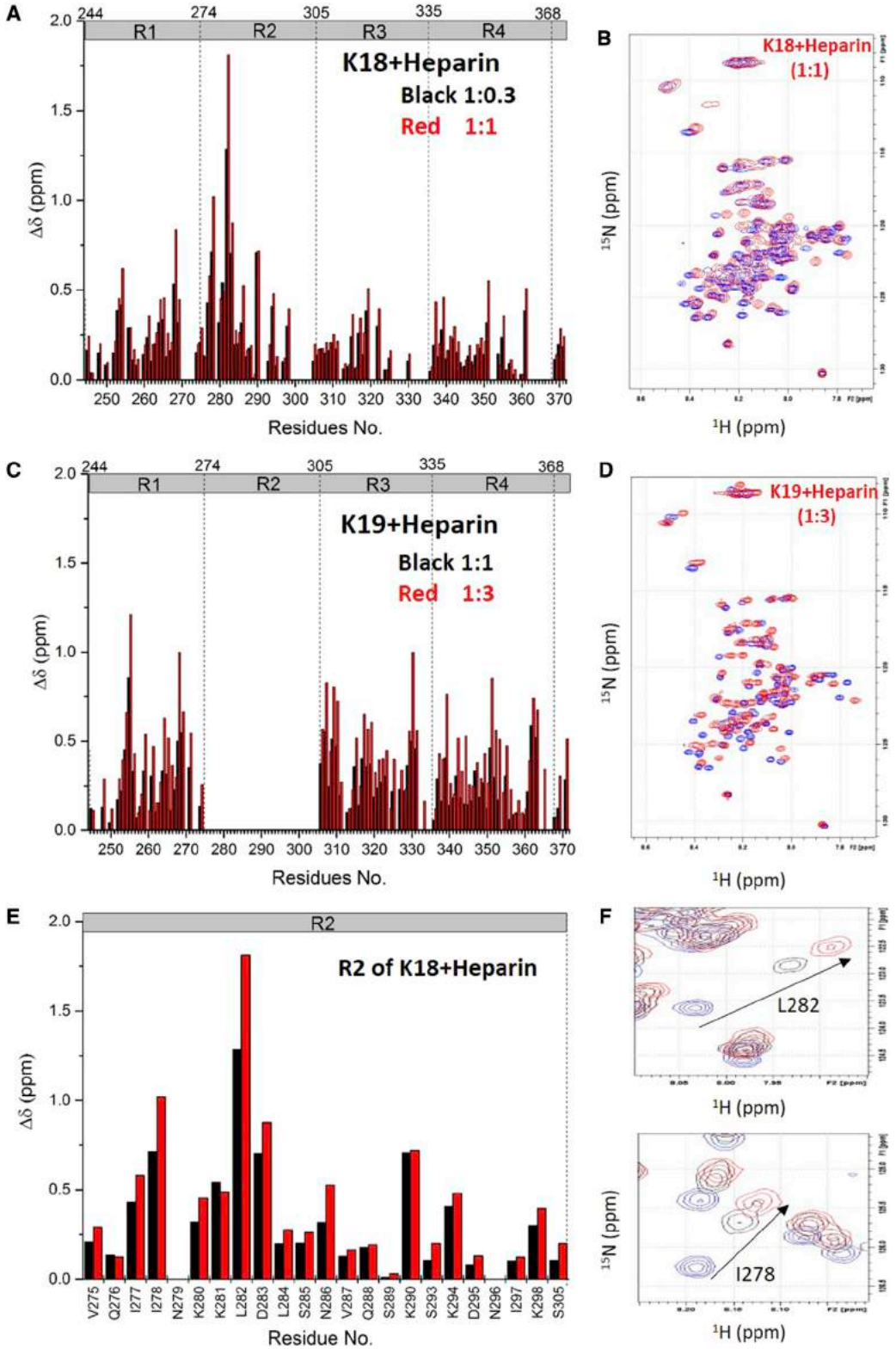

FIGURE 7 NMR titration of tau K18/K19 with heparin. (*A*) Bar graph of ^{1}H-^{15}N residue CSPs of tau K18 (0.1 mM) titrated with 0.03 mM heparin (*black bars*) and 0.1 mM heparin (*red bars*). (*B*) Overlay of the ^{1}H-^{15}N HSQC spectrum of 0.1 mM tau K18, apo (*blue*), and with 0.1 mM heparin (*red*). (*C*) Bar graph of ^{1}H-^{15}N CSPs of tau K19 (0.1 mM) titrated with 0.1 mM heparin (*black bars*) and 0.3 mM heparin (*red bars*). (*D*) Overlay of the ^{1}H-^{15}N HSQC spectrum of 0.1 mM tau K19, apo (*blue*), and in the presence of 0.3 mM heparin (*red*). (*E*) Zoom-in of (*A*) in the R2 region of tau K18 (0.1 mM) titrated with 0.03 mM heparin (*black bars*) and 0.1 mM heparin (*red bars*). (*F*) Peak movement in HSQC for the two residues with the largest CSP, I278, and L282, in the R2 domain of tau K18 (0.1 mM) titrated with 0.03 mM heparin (*black*) and 0.1 mM heparin (*red*). To see this figure in color, go online.

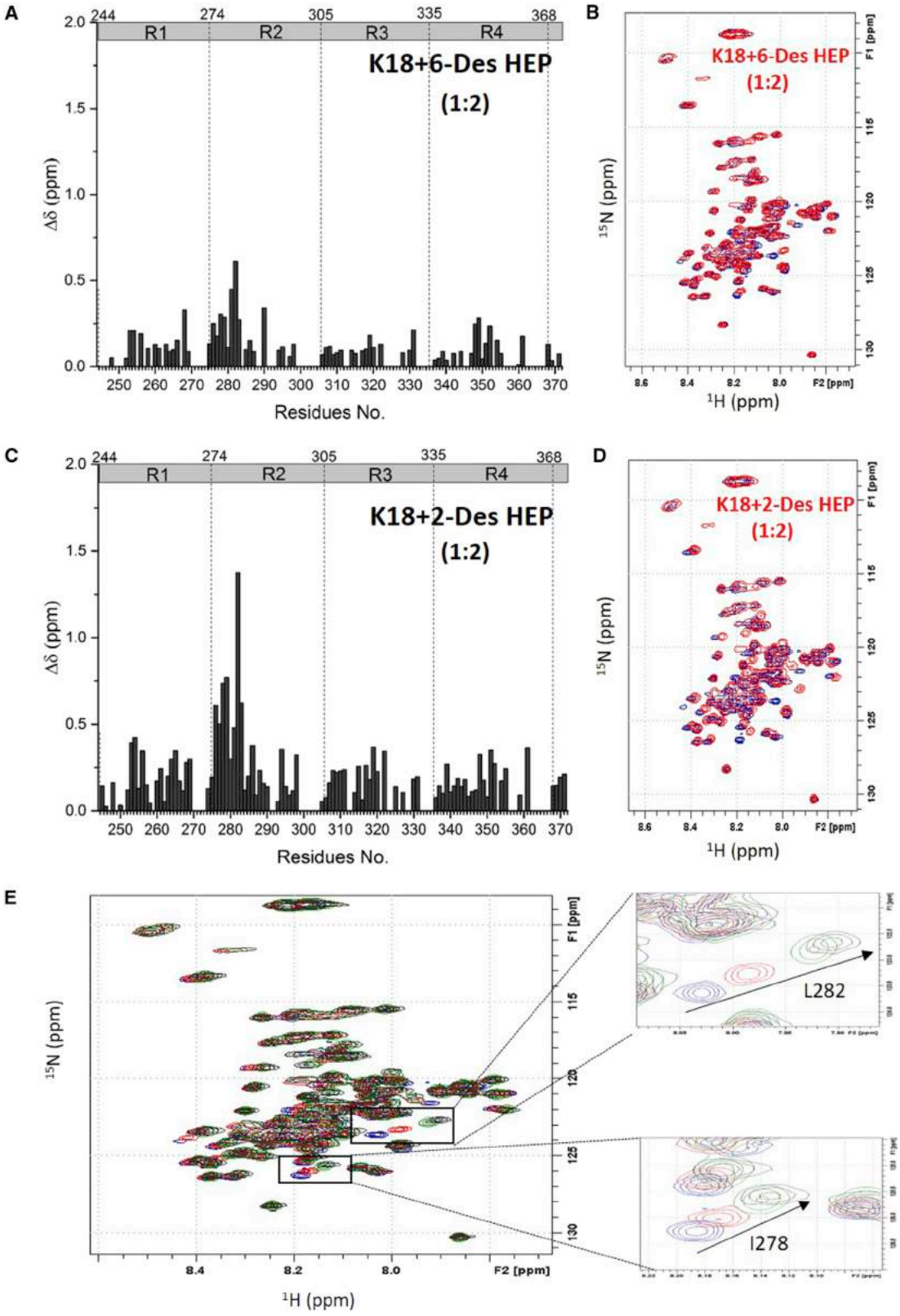

FIGURE 8 NMR titration of tau K18 with 6-Des HEP and 2-Des HEP. (*A*) CSP of tau K18 (0.1 mM) titrated with 0.2 mM 6-Des HEP. (*B*) Overlay of the ^{1}H-^{15}N HSQC spectrum of 0.1 mM tau K18, apo (*blue*), and in the presence of 0.2 mM 6-Des HEP (*red*). (*C*) Bar graph of ^{1}H-^{15}N CSP of tau K18 (0.1 mM) titrated with 0.2 mM 2-Des HEP. (*D*) Overlay of the ^{1}H-^{15}N HSQC spectrum of 0.1 mM apo tau K18 (*blue*) and K18 with 0.2 mM 2-Des HEP (*red*). (*E*) Overlay of the ^{1}H-^{15}N HSQC spectrum of 0.1 mM tau K18 (*blue*) titrated with 0.2 mM 6-Des HEP (*red*), 0.2 mM 2-Des HEP (*green*), and 0.2 mM heparin (*black*). To see this figure in color, go online.

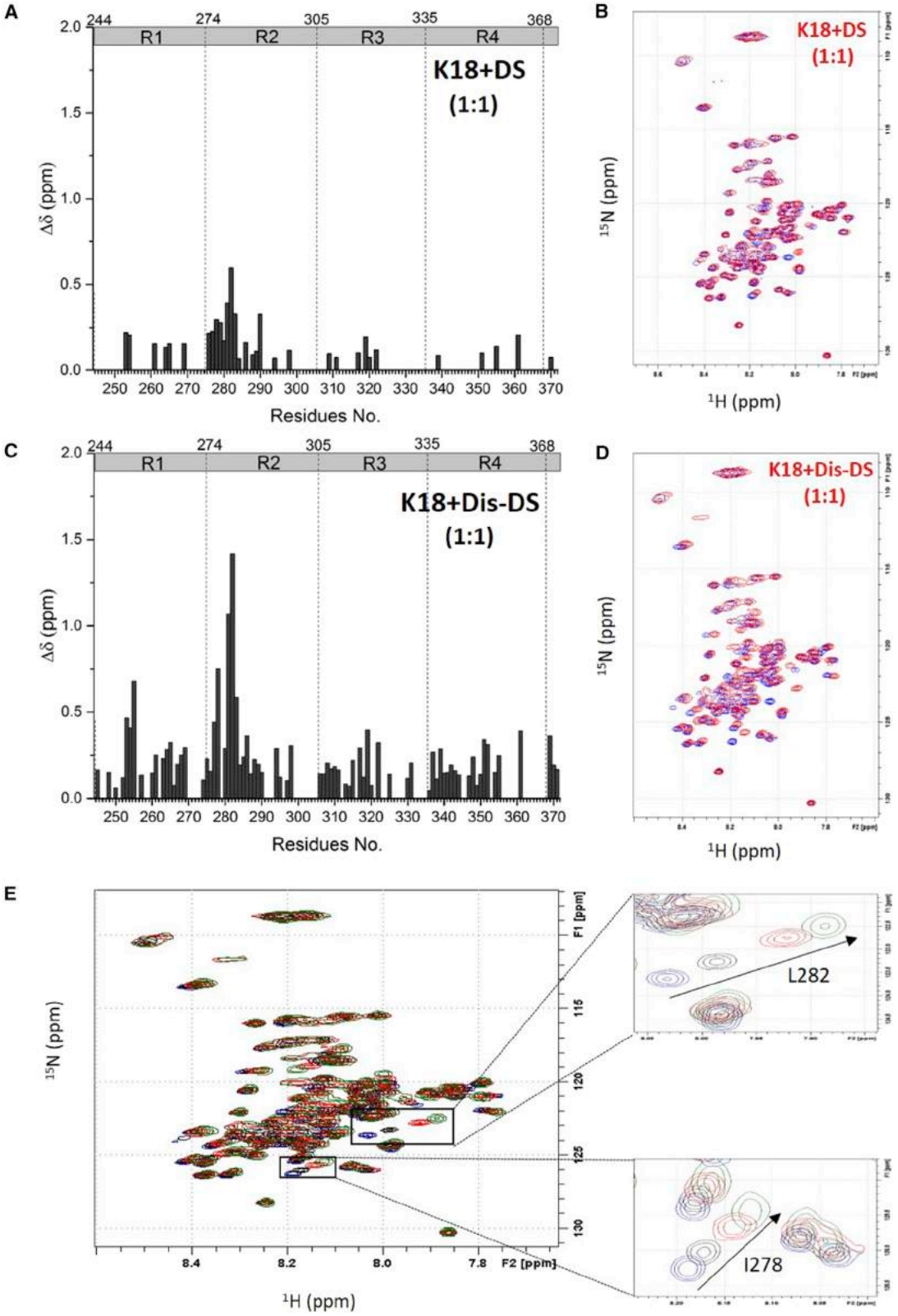

FIGURE 9 NMR titration of tau K18 with DS/Dis-DS. (*A*) CSP of tau K18 (0.1 mM) titrated with 0.1 mM DS. (*B*) Overlay of the ^{1}H-^{15}N HSQC spectrum of 0.1 mM tau K18, apo (*blue*) and in the presence of 0.1 mM DS (*red*). (*C*) Bar graph of the ^{1}H-^{15}N residue chemical shifts of tau K18 (0.1 mM) titrated with 0.1 mM Dis-DS. (*D*) Overlay of the ^{1}H-^{15}N HSQC spectrum of 0.1 mM apo tau K18 (*blue*) and K18 with 0.1 mM Dis-DS (*red*). (*E*) Overlay of the ^{1}H-^{15}N HSQC spectrum of 0.1 mM tau K18 (*blue*) titrated with 0.1 mM DS (*black*), 0.1 mM Dis-DS (*red*), and 0.1 mM heparin (*green*) in sequence, showing increasing binding affinity from DS to Dis-DS to heparin. To see this figure in color, go online.

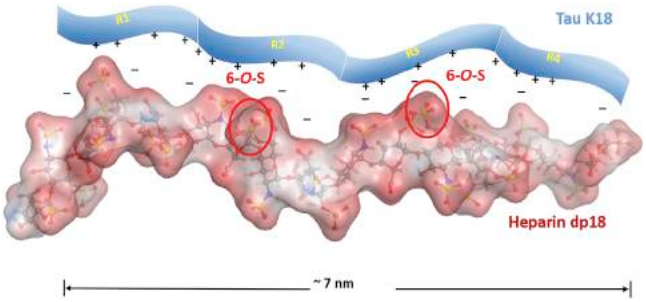

FIGURE 10 Model of tau binding to heparin. The heparin dp18 conformation is based on PDB structure 3irj, with two 6-*O*-sulfo groups highlighted. To see this figure in color, go online.

Model for tau binding to GAGs

When we examine the structure-activity relationship from the protein side, tau appears to remain disordered in its complex with heparin. This is supported by three observations. First, neither the unbound nor the GAG-bound form of tau shows an ordered structure, as demonstrated by the poor dispersion in the amide proton NMR spectrum (Fig. 7). Second, based on direct SPR measurements, K18, containing the R1–R4 domains, binds tighter than K19, which contains the R1, R3, and R4 domains. Third, based on competitive SPR measurements with heparin fragments of different lengths, the GAG binding site for tau appears to be quite large, requiring a full-length heparin chain for maximum K19 binding and a large dp18 heparin oligosaccharide chain for optimal K18 binding. The end-to-end distance for dp18 is ~7 nm in PDB structure 3irj, roughly matching the radius of gyration of K18 at 3.4 nm (41). When we examine the binding site from the GAG side, based on direct binding studies using SPR, the GAG appears to require a high degree of sulfation, i.e., two or more sulfo groups per disaccharide residue. SPR and NMR using chemically modified GAGs showed that the presence of 6-*O*-sulfo groups improves GAG binding to tau, and the GAG binding site is quite large. Finally, tau-GAG binding primarily involves ionic interactions, as it is easily abrogated by the addition of salt. A model for GAG-tau binding consistent with all of these experimental observations is shown in Fig. 10.

Tau hyperphosphorylation plays crucial roles in AD, as PHFs isolated from neurofibrillary tangles in AD brains have two to three times more phosphorylation than normal tau proteins. Hyperphosphorylated tau is thought to dissociate from MTs and to initiate tau aggregation. Nevertheless, most phosphorylation sites cluster in the proline-rich region and/or in the extreme C-terminus of tau, with few phosphorylation sites within MTBR (42). Within the MTBR region, only Ser262 and Ser356 are the targets of MT affinity-regulating kinase (43). Although Ser262 and Ser356 phosphorylation indeed disrupts tau MT assembly, phosphorylation of these two sites reduces heparin-induced PHF formation (44). NMR analyses in the literature (45) and here confirm the absence of a global structural modification due to these phosphorylation events. The electrostatic nature of the tau-heparin interaction would therefore suggest that phosphorylation near the heparin binding site will weaken the heparin-tau interaction and/or alter the mode of binding, and likely inhibit heparin-induced aggregation.

CONCLUSION

Although the interaction between tau and heparin has been extensively studied due to their importance in AD, little is known about the structural determinants of heparin for this interaction. Here, we used SPR and NMR to demonstrate the crucial role of 6-*O*-sulfation in this interaction, which to our knowledge has never been shown before. Specific sulfo groups are known to be important for GAG interactions and activity, such as the 3-*O*-sulfo group on residue III in a heparin pentasaccharide in binding antithrombin III (ATIII) (46), and the so-called sulfation code in CS (47). 3-*O*-sulfation has also been proposed to be important for the heparin-tau interaction (23); however, this was not examined in this study. The 6-*O*-sulfo group may not be as important for other GAG-tau interactions. The degree of sulfation is still the most important factor in the interaction between tau and GAGs. To the best of our knowledge, the current study provides novel insight into the tau-GAG interaction, which will contribute to a fundamental understanding of AD and the development of therapeutic treatments for this disease.

AUTHOR CONTRIBUTIONS

J.Z., F.Z., C.W., R.J.L., and G.L. designed research. J.Z., A.Z., and Q.L. performed research. I.H. and D.E. contributed analytical tools. J.Z., F.Z., C.W., R.J.L., P.T., G.L., and D.E. analyzed data. J.Z., F.Z., and C.W. wrote the manuscript.

ACKNOWLEDGMENTS

This work was supported by grants from the Rensselaer Polytechnic Institute's Knowledge and Innovation Program (to P.M.T., R.J.L., F.Z., and C.W.), the National Institutes of Health (AG019391 and AG025440 to D.E., and R01GM104130 to P.M.T.), and the Richard Baruch M.D. Chair (to P.M.T.).

REFERENCES

1. Weingarten, M. D., A. H. Lockwood, …, M. W. Kirschner. 1975. A protein factor essential for microtubule assembly. *Proc. Natl. Acad. Sci. USA.* 72:1858–1862.
2. Schoenfeld, T. A., and R. A. Obar. 1994. Diverse distribution and function of fibrous microtubule-associated proteins in the nervous system. *Int. Rev. Cytol.* 151:67–137.
3. Trojanowski, J. Q., and V. M. Lee. 2005. Pathological tau: a loss of normal function or a gain in toxicity? *Nat. Neurosci.* 8:1136–1137.
4. Iqbal, K., Adel. C. Alonso, …, I. Grundke-Iqba. 2003. Alzheimer neurofibrillary degeneration: therapeutic targets and high-throughput assays. *J. Mol. Neurosci.* 20:425–429.

5. Mandelkow, E. M., and E. Mandelkow. 2012. Biochemistry and cell biology of tau protein in neurofibrillary degeneration. *Cold Spring Harb. Perspect. Med.* 2:a006247.
6. Ren, Y., and N. Sahara. 2014. Characteristics of tau oligomers. *Front Neurol.* 4:102.
7. Wille, H., G. Drewes, …, E. Mandelkow. 1992. Alzheimer-like paired helical filaments and antiparallel dimers formed from microtubule-associated protein tau in vitro. *J. Cell Biol.* 118:573–584.
8. Buée, L., T. Bussière, …, P. R. Hof. 2000. Tau protein isoforms, phosphorylation and role in neurodegenerative disorders. *Brain Res. Brain Res. Rev.* 33:95–130.
9. Ihara, Y., N. Nukina, …, M. Ogawara. 1986. Phosphorylated tau protein is integrated into paired helical filaments in Alzheimer's disease. *J. Biochem.* 99:1807–1810.
10. Alonso, A., T. Zaidi, …, K. Iqbal. 2001. Hyperphosphorylation induces self-assembly of tau into tangles of paired helical filaments/straight filaments. *Proc. Natl. Acad. Sci. USA.* 98:6923–6928.
11. Kampers, T., P. Friedhoff, …, E. Mandelkow. 1996. RNA stimulates aggregation of microtubule-associated protein tau into Alzheimer-like paired helical filaments. *FEBS Lett.* 399:344–349.
12. Wilson, D. M., and L. I. Binder. 1997. Free fatty acids stimulate the polymerization of tau and amyloid beta peptides. In vitro evidence for a common effector of pathogenesis in Alzheimer's disease. *Am. J. Pathol.* 150:2181–2195.
13. Friedhoff, P., A. Schneider, …, E. Mandelkow. 1998. Rapid assembly of Alzheimer-like paired helical filaments from microtubule-associated protein tau monitored by fluorescence in solution. *Biochemistry.* 37:10223–10230.
14. Goedert, M., R. Jakes, …, R. A. Crowther. 1996. Assembly of microtubule-associated protein tau into Alzheimer-like filaments induced by sulphated glycosaminoglycans. *Nature.* 383:550–553.
15. Holmes, B. B., S. L. DeVos, …, M. I. Diamond. 2013. Heparan sulfate proteoglycans mediate internalization and propagation of specific proteopathic seeds. *Proc. Natl. Acad. Sci. USA.* 110:E3138–E3147.
16. Linhardt, R. J., R. J. Kerns, and I. R. Vlahov. 1996. Heparin and heparin oligosaccharides: preparation, analysis, application and biological activities. *In* Biochemical Functions and Biotechnology of Natural and Artificial Polymers. M. Yalpani, editor. Science Publishers, Mt. Prospect, IL, pp. 46–62.
17. Linhardt, R. J., and T. Toida. 2004. Role of glycosaminoglycans in cellular communication. *Acc. Chem. Res.* 37:431–438.
18. Iozzo, R. V., J. J. Zoeller, and A. Nyström. 2009. Basement membrane proteoglycans: modulators par excellence of cancer growth and angiogenesis. *Mol. Cells.* 27:503–513.
19. Capila, I., and R. J. Linhardt. 2002. Heparin-protein interactions. *Angew. Chem. Int. Ed. Engl.* 41:391–412.
20. Mukrasch, M. D., J. Biernat, …, M. Zweckstetter. 2005. Sites of tau important for aggregation populate β-structure and bind to microtubules and polyanions. *J. Biol. Chem.* 280:24978–24986.
21. Sibille, N., A. Sillen, …, G. Lippens. 2006. Structural impact of heparin binding to full-length Tau as studied by NMR spectroscopy. *Biochemistry.* 45:12560–12572.
22. Mukrasch, M. D., M. von Bergen, …, M. Zweckstetter. 2007. The "jaws" of the tau-microtubule interaction. *J. Biol. Chem.* 282:12230–12239.
23. Sepulveda-Diaz, J. E., S. M. Alavi Naini, …, D. Papy-Garcia. 2015. HS3ST2 expression is critical for the abnormal phosphorylation of tau in Alzheimer's disease-related tau pathology. *Brain.* 138:1339–1354.
24. Jangholi, A., M. R. Ashrafi-Kooshk, …, R. Khodarahmi. 2016. Appraisal of role of the polyanionic inducer length on amyloid formation by 412-residue 1N4R Tau protein: a comparative study. *Arch. Biochem. Biophys.* 609:1–19.
25. Barré, P., and D. Eliezer. 2013. Structural transitions in tau k18 on micelle binding suggest a hierarchy in the efficacy of individual microtubule-binding repeats in filament nucleation. *Protein Sci.* 22:1037–1048.
26. Eliezer, D., P. Barré, …, L. Heend. 2005. Residual structure in the repeat domain of tau: echoes of microtubule binding and paired helical filament formation. *Biochemistry.* 44:1026–1036.
27. Yates, E. A., F. Santini, …, B. Casu. 1996. ^{1}H and ^{13}C NMR spectral assignments of the major sequences of twelve systematically modified heparin derivatives. *Carbohydr. Res.* 294:15–27.
28. Weyers, A., B. Yang, …, R. J. Linhardt. 2013. Isolation of bovine corneal keratan sulfate and its growth factor and morphogen binding. *FEBS J.* 280:2285–2293.
29. Pervin, A., C. Gallo, …, R. J. Linhardt. 1995. Preparation and structural characterization of large heparin-derived oligosaccharides. *Glycobiology.* 5:83–95.
30. Hernaiz, M., J. Liu, …, R. J. Linhardt. 2000. Enzymatic modification of heparan sulfate on a biochip promotes its interaction with antithrombin III. *Biochem. Biophys. Res. Commun.* 276:292–297.
31. Zhao, J., X. Liu, …, R. J. Linhardt. 2016. Kinetic and structural studies of interactions between glycosaminoglycans and langerin. *Biochemistry.* 55:4552–4559.
32. Zhang, F., J. Aguilera, …, R. J. Linhardt. 2013. Characterization of interactions between heparin/glycosaminoglycan and adeno-associated virus. *Biochemistry.* 52:6275–6285.
33. Zhang, F., Z. Zhang, …, R. J. Linhardt. 2009. Compositional analysis of heparin/heparan sulfate interacting with fibroblast growth factor.fibroblast growth factor receptor complexes. *Biochemistry.* 48:8379–8386.
34. Trzeciakiewicz, H., J. O. Esteves-Villanueva, …, S. Martić. 2015. Electrochemistry of heparin binding to tau protein on Au surfaces. *Electrochim. Acta.* 162:24–30.
35. Schweers, O., E. Schönbrunn-Hanebeck, …, E. Mandelkow. 1994. Structural studies of tau protein and Alzheimer paired helical filaments show no evidence for beta-structure. *J. Biol. Chem.* 269:24290–24297.
36. von Bergen, M., P. Friedhoff, …, E. Mandelkow. 2000. Assembly of tau protein into Alzheimer paired helical filaments depends on a local sequence motif ((306)VQIVYK(311)) forming beta structure. *Proc. Natl. Acad. Sci. USA.* 97:5129–5134.
37. Smet, C., A. Leroy, …, G. Lippens. 2004. Accepting its random coil nature allows a partial NMR assignment of the neuronal Tau protein. *ChemBioChem.* 5:1639–1646.
38. Qi, H., F. X. Cantrelle, …, I. Landrieu. 2015. Nuclear magnetic resonance spectroscopy characterization of interaction of Tau with DNA and its regulation by phosphorylation. *Biochemistry.* 54:1525–1533.
39. Lippens, G., I. Landrieu, …, J. Lopez. 2016. NMR meets Tau: insights into its function and pathology. *Biomolecules.* 6:E28.
40. Nishiura, C., K. Takeuchi, …, T. Ishida. 2010. Importance of Tyr310 residue in the third repeat of microtubule binding domain for filament formation of tau protein. *J. Biochem.* 147:405–414.
41. Mylonas, E., A. Hascher, …, D. I. Svergun. 2008. Domain conformation of tau protein studied by solution small-angle X-ray scattering. *Biochemistry.* 47:10345–10353.
42. Noble, W., D. P. Hanger, …, S. Lovestone. 2013. The importance of tau phosphorylation for neurodegenerative diseases. *Front. Neurol.* 4:83.
43. Drewes, G., A. Ebneth, …, E. Mandelkow. 1997. MARK, a novel family of protein kinases that phosphorylate microtubule-associated proteins and trigger microtubule disruption. *Cell.* 89:297–308.
44. Schneider, A., J. Biernat, …, E. M. Mandelkow. 1999. Phosphorylation that detaches tau protein from microtubules (Ser262, Ser214) also protects it against aggregation into Alzheimer paired helical filaments. *Biochemistry.* 38:3549–3558.
45. Schwalbe, M., J. Biernat, …, M. Zweckstetter. 2013. Phosphorylation of human Tau protein by microtubule affinity-regulating kinase 2. *Biochemistry.* 52:9068–9079.
46. Atha, D. H., J. C. Lormeau, …, J. Choay. 1987. Contribution of 3-O- and 6-O-sulfated glucosamine residues in the heparin-induced conformational change in antithrombin III. *Biochemistry.* 26:6454–6461.
47. Gama, C. I., S. E. Tully, …, L. C. Hsieh-Wilson. 2006. Sulfation patterns of glycosaminoglycans encode molecular recognition and activity. *Nat. Chem. Biol.* 2:467–473.